



# Production and characterization of lightweight aggregates from municipal solid waste incineration fly-ash through single- and double-step pelletization process

Alberto Ferraro<sup>a</sup>, Vilma Ducman<sup>b</sup>, Francesco Colangelo<sup>c,d</sup>, Lidija Korat<sup>b</sup>, Danilo Spasiano<sup>a</sup>, Ilenia Farina<sup>c,d,\*</sup>

<sup>a</sup> Department of Civil, Environmental, Land, Building Engineering and Chemistry, Polytechnic University of Bari, Via E. Orabona 4, 70125, Bari, Italy

<sup>b</sup> Slovenian National Building and Civil Engineering Institute (ZAG), Dimičeva ulica 12, 1000, Ljubljana, Slovenia

<sup>c</sup> Department of Engineering, University of Naples "Parthenope", Centro Direzionale di Napoli, Isola C4, 80143, Naples, Italy

<sup>d</sup> INSTM Research Unit, University Parthenope of Naples, Centro Direzionale, Is. C4, 80143, Naples, Italy

## ARTICLE INFO

Handling Editor: Maria Teresa Moreira

### Keywords:

Washing pre-treatment  
MSWI fly-Ash  
Cold-bonding pelletization  
Lightweight aggregates

## ABSTRACT

The performance of a cold-bonding pelletization process was investigated for lightweight aggregates (LWAs) production from municipal solid waste incineration (MSWI) fly-ash (FA), by including multiple waste materials in the aggregate mixture. Before pelletization, FA was pre-treated by washing with water, which led to a reduction of chloride (66.79%) and sulphate (25.30%) content. This was further confirmed by XRF and XRD analyses, which showed a reduction of chloride elements and the content of chlorine crystalline phases. The pelletization process was carried out using both single- and double-step methods. For single-step pelletization, all the mixtures contained 80% FA, combined with various compositions of cement (5, 10, and 15%) and granulated blast furnace slag (GBFS) (5, 10, and 15%). For the double-step pelletization 30% of cement and 70% of marble sludge (MS) were added to each of the previous mixtures. The apparent density of all the aggregates varied between 1.60 and 1.87 g cm<sup>-3</sup>, suggesting their suitability to be classified as LWAs. Aggregates produced from double-step pelletization showed improved characteristics, with water absorption capacity and open porosity generally lower compared to the corresponding aggregates from the single-step pelletization. The best values of compressive (crushing) strength (almost 11 MPa) were observed for double-step pelletization aggregates with initial cement: GBFS mixture of 15%:5%. Results from leaching tests showed an overall significant release of chloride and sulphate. Nevertheless, leaching from double-step pelletization aggregates was reduced by 1.73-4.02 times for chloride and 1.58-5.67 times for sulphate, further suggesting that better performances are achievable through the addition of an aggregate second layer.

## 1. Introduction

The incineration process represents a feasible technical approach to the treatment of municipal solid wastes, benefitting from the advantage of significant reductions in waste mass and volume (Kirkelund et al., 2020). Accordingly, incineration can be considered as a practical alternative to the disposal of municipal solid waste in landfills, thus overcoming several related environmental issues. Indeed, incineration practice for sustainable municipal solid waste management must require the development of efficient technologies for the i) waste volumetric reduction, ii) optimal heat and materials recovery and iii) resulting flue

gas treatment to comply with gas emission regulation limits (Makarichi et al., 2018). Besides this, one of the most concerning drawbacks of municipal solid waste incineration (MSWI) is the formation of further by-products that display toxic and hazardous characteristics (de Gisi et al., 2018).

Among these, MSWI fly-ash (FA) is identified as a non-chemically inert and hazardous waste, which poses a high risk to the environment due to a significant content of heavy metals (HMs), chloride, and sulphate (Loginova et al., 2019). Furthermore, the leaching phenomena of HMs, resulting from the presence of soluble metal salts and chlorides, poses an additional risk to the health of any organisms potentially

\* Corresponding author. Department of Engineering, University of Naples "Parthenope", Centro Direzionale di Napoli, Isola C4, 80143, Naples, Italy.  
E-mail address: [ilenia.farina@uniparthenope.it](mailto:ilenia.farina@uniparthenope.it) (I. Farina).

exposed (Race, 2017; Yang et al., 2017). The remediation and safe disposal of MSWI FA has therefore become an imperative issue, leading various researchers to focus on the application of feasible treatment approaches in this field. In this perspective, the solidification/stabilization (S/S) process proved to be a suitable application for the treatment of MSWI FA, enabling waste material to be contained in a solidified matrix and achieve chemical stability, thus avoiding any potential leaching phenomena (Barjoveanu et al., 2018; Senneca et al., 2020). Moreover, a common practice in several investigations has been to involve different pre-treatment typologies (i.e. washing, electrochemical, thermal) in order to initially decrease the content of contaminants in MSWI FA and further enhance the stabilization process (Ferraro et al., 2019).

These days, a well-assessed S/S methodology is represented by cold-bonding pelletization. This process is generally carried out through a rotating plate device, allowing the formation of pelletized aggregates from moist materials (such as waste materials) through gravitational and centrifugal forces (Ferraro et al., 2021). In general, a further advantage arising from waste stabilization within pellets is the concurrent production of lightweight aggregates (LWAs) (Rehman et al., 2020), which have the potential to be reused in further applications such as in the manufacture of lightweight concrete (LWC). A further practice for the production of LWAs is represented by the aggregates sintering through rotary kiln after the pellets formation. In this case, despite a very fast production of useable LWAs, it should be taken into account that sintering represents a more energy intensive treatment than the cold-bonding process also due to the higher temperature involved in the first compared to the latter. Moreover, at very high temperature values during sintering, excess gas can be produced leading to the increase of aggregates porosity (Ayati et al., 2018). Finally, it is worth mentioning that secondary pollution in terms of gaseous emissions could result from sintering application necessarily requiring the implementation of suitable flue gas cleaning systems (Ayati et al., 2018; Thomas and Harilal, 2015).

Accordingly, several scientific studies have been carried out to investigate the suitability of cold-bonding pelletization for various types of waste (Malenšek et al., 2015) and, in particular, for MSWI FA. For example, besides investigating the formation of pellets by mixing FA with cement (Chi et al., 2003; Franković et al., 2017), different studies have tested the potential efficacy of various binders, such as bentonite, kaolinite, furnace slag, alkaline activator, and lime (Bui et al., 2012b; Ferone et al., 2013; Manikandan and Ramamurthy, 2007; Perumal and Sivakumar, 2014). Further applications aimed at improving the mechanical properties of aggregates by combining binary or ternary mixtures of various wastes with FA in the pellet mix-design have been reported. Examples have been provided by researchers using granulated blast furnace slag (GBFS), bottom ash, paper sludge ash, and coal FA as additives to the mixture in the production of FA aggregates (Hwang and Tran, 2015; Tang and Brouwers, 2017). In another study, different combinations aimed at manufacturing artificial aggregates from FA, cement, hydrated lime, GBFS, silica fume, metakaolin, sodium bentonite and calcium bentonite were tested (Valia and Murugan, 2020). Few studies evaluating this approach in the production of LWAs from MSWI FA have, however, been reported. Even less investigated is the performance of cold-bonding pelletization through double-step pelletization. In a previous study, the formation of a second outer layer on granules (made by cement:coal FA with a 1:1 ratio in an amount equivalent to 40% of the granule weight) significantly enhanced the mechanical characteristics of the aggregates (Colangelo et al., 2015).

While the use of multiple types of waste and technical strategies is important both to recycle more material and concurrently improve the properties of cold-bonded aggregates, careful optimization of the entire process is also fundamental in order to achieve a suitable compromise between the efficiency of the process and economical factors. In these terms, an important factor is minimizing the amount of cement binder involved in the production of aggregates, consequently saving costs, and

leading to a process with lower environmental impact. In the present work, the cold-bonding pelletization technique was performed to stabilize MSWI FA, using various mix-designs of a ternary mixture (MSWI FA:cement:GBFS) for the production of aggregates. In particular, the addition of different amounts of cement, at low percentages (i.e. 5, 10, and 15%), was investigated, using a fixed amount of FA (80%) and various percentages of GBFS (i.e. 15, 10, and 5%). A preliminary water-washing treatment was performed on MSWI FA in order to decrease the high amount of soluble salts, thereby improving the characteristics of the FA for the pelletization phase. The aggregates produced further underwent a second pelletization step, through the addition of a mixture of cement and marble sludge (MS), in order to develop pellets characterized by an outer layer and make a deeper comparison between single- and double-layer aggregates. Accordingly, the best operating conditions for cold-bonding pelletization were investigated with the aim of providing MSWI FA aggregates with suitable characteristics, whilst minimizing the overall costs of the process as well as the environmental impact.

## 2. Materials and methods

### 2.1. Characterization of materials

Characterization analyses were carried out in order to determine the physical-chemical properties of the waste materials. The pH of FA was determined using a pH meter (Orion 420A+, Thermo) in a mixture of FA and deionized water combined in a ratio of 1:2.5 (m/v). The HMs content of FA was determined through acid mineralization of FA samples (1 g) in aqua regia (10 mL) using a Milestone START D microwave oven. The liquid phase from acid mineralization was filtered and diluted with deionized water added up to a total volume of 100 mL. Then, further detection of HMs in the diluted samples was carried out through atomic adsorption spectrometry (AAS), using a Varian Model 55B SpectrAA (F-AAS) equipped with a flame (acetylene/air) and a deuterium lamp for background correction. The content of chloride and sulphate in the FA samples was determined by a leaching test in deionized water for 24 h, using a liquid to solid ratio of 10 (v/m). The leaching solution was then further analysed by ionic liquid chromatography.

The particle size distribution of FA, GBFS, and MS was determined using a Malvern Instrument Mastersizer 2000 laser scattering analyser (with a particle observation range between 0.02 and 2000  $\mu\text{m}$ ). Scanning electron microscopy (SEM) through a PhenomProX scanning electron microscope was performed on FA, GBFS, and MS in order to determine their microstructure. The fraction of volatile components within FA and MS, as well as their stability, was evaluated through thermogravimetric analysis (TGA) using a Mettler Toledo TGA/DSC 2 STAR<sup>®</sup> System. Finally, X-ray diffraction (XRD) and X-ray fluorescence spectroscopy (XRF) analyses were performed on FA, GBFS, and MS in order to identify the crystalline structure and material components, respectively. The binder used for the production of granules was CEM II/A-L 42.5R cement (UNI EN 197-1, 2011). As for the waste materials, SEM, TGA, XRD, and XRF analyses were also carried out for characterization of the cement.

### 2.2. The washing pre-treatment of fly-ash

Washing pre-treatment was carried out on FA prior to its use in the pelletization process, primarily in order to reduce the content of chloride and sulphate. With this aim, 19 kg of FA was washed with deionized water in a continuous stirred-tank reactor (CSTR). The pre-treatment was carried out using a two-step washing process, with each step using a liquid to solid ratio equal to 2.5 and a retention time of 1.5 h. The operating conditions for the washing pre-treatment were selected on the basis of process optimization tests performed in previous works (Colangelo et al., 2012, 2015).

After pre-treatment, the washed FA (W-FA) was collected through

filtration and dried at 45 °C prior to further analyses or use in the cold-bonding process. Part of the W-FA was used for particle size distribution, SEM, TGA, and XRD analyses, in order to provide a deeper characteristics comparison with the untreated FA.

### 2.3. Cold-bonding process

#### 2.3.1. Production of aggregates

The W-FA was then used for the further production of granular aggregates through the cold-bonding pelletization process. The latter was performed using a pilot-scale granulator equipped with a rotating plate of 80 cm diameter. The speed of rotation and inclination angle of the plate were fixed to 45 rpm and 45°, respectively. Three different mixtures were investigated, with varying percentages of cement and GBFS (Table 1). The final mixture proportions were set after preliminary tests carried out by changing the percentages of the constituent materials. The involvement of a fixed percentage of W-FA in all the mixtures was selected in order to provide a proper comparison among all the produced aggregates. All mixtures manufactured by the cold-bonding process underwent a second pelletization step. Different percentages of the constituent materials were preliminary tested also in the double-step pelletization and the cement:MS ratio equal to 30:70 was selected among the previously verified values in order to minimize the cement content.

Average water percentage used during the aggregates production was equal to  $22 \pm 0.7\%$  and  $14 \pm 2.7\%$  for single- and double-step pelletization processes, respectively. These percentages were evaluated on the weight of the total mixture in the single-step pelletization and the weight of the mixture required for the outer layer formation in the double-step pelletization. Figs. S1a and b of the supplementary material (SM) display the pilot-scale granulator while running the single- and double-step pelletization tests, respectively. All the aggregates produced were cured for 28 days at room temperature and a relative humidity of 95% in order to achieve a hardness suitable for further characterization tests.

#### 2.3.2. Characterization of the physical-chemical and mechanical properties of aggregates

After the curing phase, all the aggregates were characterized in terms of their physical-chemical and mechanical properties. The particle size distribution of the aggregates was determined according to the procedure outlined in standard UNI EN 933-1 (2012). Apparent density (further indicated as density), porosity, volume, and water absorption capacity (WAC) were determined according to the method reported by Colangelo et al. (2015). In brief, the aggregates were soaked in water at  $20 \pm 2$  °C for 24 h and then the surface was wiped with a moist cloth. Density and open porosity were determined after measuring the weight of the same aggregates dried at 105 °C. WAC was determined according to equation (1):

$$WAC = 100 \cdot \frac{m_w - m_d}{m_d} \quad \text{Equation 1}$$

with  $m_w$  and  $m_d$  representing the mass of the water saturated aggregates

**Table 1**

Mixture composition of aggregates obtained from single- and double-step pelletization.

Test	Single-step pelletization			Double-step pelletization	
	Cement (%)	GBFS (%)	FA (%)	Cement (%)	MS (%)
S-C5S15	5	15	80	–	–
S-C10S10	10	10	80	–	–
S-C15S5	15	5	80	–	–
D-C5S15	5	15	80	30	70
D-C10S10	10	10	80	30	70
D-C15S5	15	5	80	30	70

and the mass of the dried aggregates, respectively. Test of impact resistance was carried out on aggregates with a particle size ranging from 10 to 14 mm, in accordance with the standard UNI EN 12620 (2013). This test was performed on a heap of aggregates by means of a Matest press. After the aggregates had been crushed through the impact of the press (15 consecutive times), the amount of material able to pass through a 2 mm sieve was weighed and the passing percentage was determined. The compressive (crushing) strength of aggregates was determined according to the standard UNI EN 13055-1 (2002) using a 3000 kN Controls® MC60 press.

X-ray micro-computed tomography (micro-CT) using an XRadia CT-400 tomograph (XRadia, Concord, CA, USA) was performed to investigate the structural properties of the aggregates. The scanning parameters were as follows: beam energy and intensity were set to 80 kV and 70 μA, respectively, 1600 projection images were acquired at an exposure time of 9 s per projection, and the resolution of one pixel was 15 μm. Avizo Fire three-dimensional (3D)-image analysis software (Thermo Scientific™ Avizo™ Software, Thermo Fisher Scientific, Waltham, MA, USA) was used to reconstruct the 3D internal pore structure of the aggregates, as well as to estimate the overall porosity (Korat et al., 2013). Low vacuum scanning electron microscopy (LV SEM) was used to analyse the cross section of the aggregates, which had been previously analysed by X-ray micro-CT. Half of each granule was used for LV SEM analysis and the other half for mercury intrusion porosimetry (MIP). The microstructures of the aggregates were analysed using a JEOL 5500 LV scanning electron microscope in low vacuum mode. The porosity and pore size distribution were determined on half of the granules, using an AutoPore IV 9510 Hg-porosimeter from Micromeritics. Pressure was applied up to 414 MPa.

Finally, leaching tests were carried out in order to quantify the potential release of chloride, sulphate, and HMs from the stabilized aggregates. These tests were carried out in accordance to the procedure outlined in standard UNI EN 10802 (2013), with a single-washing step of 24 h and a liquid to solid ratio equal to 10. Following the tests, the aggregates were separated from the leaching solution and dried at 105 °C for further weight determination in order to determine any mass loss. The leaching solution was analysed by atomic adsorption spectrometry for the determination of HMs, and by ionic liquid chromatography for the determination of chloride and sulphate.

## 3. Results and discussion

### 3.1. Characterization of cement, granulated blast furnace slag and marble sludge

Results from the XRF analysis of cement, GBFS, and MS are reported in Table S1 of the SM. In general, results displayed typical cement composition related to the manufacturing of cement. Almost 90 wt% of the GBFS was composed of iron, aluminium, magnesium, and silicon oxides, the presence of which can be ascribed to the oxidation of metal components during the steelwork manufacturing process. On the contrary, MS was mainly characterized by calcium oxide (almost 50 wt%), with a lower presence of CO (22.74 wt%) and iron, aluminium, magnesium, and silicon oxides (almost 30 wt%). Alite ( $\text{Ca}_3\text{SiO}_5$ ) and belite ( $\text{Ca}_2\text{SiO}_4$ ) were the main crystalline structures detected in the cement (Fig. S2a of the SM) while Wustite (FeO), Monticellite ( $\text{Ca}(\text{FeMg})\text{SiO}_4$ ), and Gehlenite ( $\text{Ca}_2\text{Al}(\text{AlSiO})\text{OH}$ ) were detected in the GBFS (Fig. S2b of the SM), which is consistent with the elemental composition identified through XRD analysis. The main crystalline structures detected in the MS were quartz ( $\text{SiO}_2$ ), calcite ( $\text{CaCO}_3$ ),  $\text{KNaAlSi}_3\text{O}_8$  and Annite ( $\text{KFeAlSi}_3\text{O}_{10}(\text{OH})_2$ ) (Fig. S2c of the SM).

Fig. S3a, b, and c in the SM report the SEM scans for cement, GBFS, and MS, respectively. It was evident from the SEM results that the cement and MS had an irregular surface and contained a higher presence of crystalline structures in comparison to the GBFS. In fact, GBFS displayed an amorphous matrix and a more porous surface. Moreover,

higher magnification of the GBFS SEM scans showed the presence of elements characterized by incomplete chemical reactions ( $\text{Fe}_2\text{O}_3 \approx 64\%$ ). TGA analysis of cement (Fig. S4a of the SM) displayed weight losses in the material at three different temperatures (120, 400, and 700 °C.) These were respectively attributed to humidity loss of the sample, the decomposition of  $\text{Ca}(\text{OH})_2$  to CaO, and the  $\text{CaCO}_3$  calcination reaction with the consequent production of CaO and  $\text{CO}_2$ . On the contrary, in the MS, weight loss was only detected at 800 °C (Fig. S4b of the SM), which was also attributed to  $\text{CaCO}_3$  calcination. Finally, single-mode particle size distribution was observed for both GBFS and MS, with the main modal values equal to 33.2 and 15.5  $\mu\text{m}$ , respectively (Figs. S5a and b of the SM).  $d_{50}$  values from the cumulative distribution were equal to 33.15 and 13.5  $\mu\text{m}$  for GBFS and MS, respectively (Figs. S5c and d of the SM).

### 3.2. Characterization of fly-ash and washed fly-ash

Table S2 of the SM reports data on the pH, elemental composition, particle size distribution, HMs content, and chloride and sulphate concentrations of both the FA and W-FA. The pH of the FA both before and after the washing pre-treatment resulted in typical alkaline values due to the high presence of metal oxides and carbonates, which generally confer a significant buffer capacity to the FA (Xinghua et al., 2016). According to the XRF data, the FA displayed a high percentage of chloride (21.20 wt%), as expected, and a lower content of sulphate (8.57 wt%). A significant reduction in the amount of chloride was observed after the washing pre-treatment, resulting in a residual percentage of 8.77%. This was confirmed by the results of total chloride concentration, which highlighted that 60590  $\text{mg kg}^{-1}$  (66.79%) had been removed. Despite the sulphate percentage in W-FA being almost constant (9.58 wt%) compared to the untreated FA, the total sulphate concentration after washing was 25.3% less. A noticeable increase in the percentage of some element within the W-FA (such as CaO) could be attributed to changes in the elemental concentration due to the reduction in mass caused by the solubilization of salts and/or the removal of oxides (such as ClO,  $\text{Na}_2\text{O}$ , and  $\text{K}_2\text{O}$ ) during the washing. Generally, a lower percentage of particles sized from 1 to 120  $\mu\text{m}$  were observed in W-FA compared to FA. This latter result suggests that washing pre-treatment led to the loss of particles lower than 120  $\mu\text{m}$ . In general, the finest particle size could provide better interparticle contact during the cold-bonding process and consequent higher mechanical properties of the produced aggregates. However, it should be taken into account that very fine particles scarcely aggregate with proper efficiency during cold-bonding practice performed at pilot-scale applications and significant amount of these loose particles can remain on the granulator bottom after the operations. According to this, the loss of particles lower than 120  $\mu\text{m}$  after the washing pre-treatment was not considered as a significant influencing factor of the cold-bonding efficiency since the granulator operating scale involved in this work.

Comparing the total concentrations of HMs before and after the washing pre-treatment only Cu showed a reduction, equating to a removal of 25.44%. Instead, Cd, Pb, Cr, and Zn, total concentration values resulted higher after the washing pre-treatment. This could be intrinsically correlated to the dissolution of soluble salts, as also observed in the XRF data for other elements, leading to a weight loss in the W-FA and more concentrated amount detectable of these HMs. The high concentration of HMs in W-FA, however, as well as the presence of chloride and sulphate, highlighted the significant danger of the FA investigated, supporting the need for a further stabilization step after washing.

Fig. 1a and b report XRD data for FA and W-FA, respectively. In accordance with the XRF analysis, FA displayed a high presence of crystalline phases, represented by calcium oxide (CaO), calcite ( $\text{CaCO}_3$ ), Portlandite ( $\text{Ca}(\text{OH})_2$ ), calcium sulphate ( $\text{Ca}(\text{SO})_4$ ), sodium chloride (NaCl), potassium chloride (KCl), calcium hydroxychloride ( $\text{CaClOH}$ ), potassium hydroxide (KOH), and quartz. The main crystalline phases

mentioned above are generally observed in MSWI FA (Zheng et al., 2011). Following the pre-treatment, the XRD data for W-FA in part displayed the presence of the same crystalline phases seen in the untreated FA (such as  $\text{CaCO}_3$ , Portlandite, and  $\text{Ca}(\text{SO})_4$ ). Moreover, due to the water washing, several hydrated species, such as syngenite ( $\text{K}_2\text{Ca}(\text{SO}_4)_2 \cdot 2\text{H}_2\text{O}$ ),  $\text{CaSO}_4 \cdot 2\text{H}_2\text{O}$ , and  $\text{Ca}(\text{ClO})_2 \cdot 3\text{H}_2\text{O}$  were detected. The washing pre-treatment could, in part, be affecting the hydraulic/pozzolanic properties of the FA useful for hydration reactions during the stabilization process. It must be highlighted, however, that the decrease in the content of soluble salts in the FA plays a significant role in the achievement of a final stabilized product with good durability characteristics. Accordingly, in the present work, the main difference with the untreated FA was the lower presence of chlorine-containing crystalline phases (such as NaCl) in the W-FA, which could be related to the dissolution of chloride salts during the washing step (Yang et al., 2017).

SEM scans for FA and W-FA are reported in Fig. 1c and d, respectively. In general, particles characterized by an irregular and coarse surface were displayed in both cases, before and after the washing pre-treatment. This can be expected, since the washing pre-treatment, carried out with water, generally has less of an impact on the morphology of particles compared to a pre-treatment of acid washing, which can lead to a greater removal of insoluble species in addition to those that are water soluble (Hu et al., 2015). It is, however, worth noticing, that W-FA was composed of larger-sized particles compared to the untreated FA, as a result of the occurrence of hydration reactions. This was consistent with the particle size distribution results, which highlighted an increase in the particle distribution above 120  $\mu\text{m}$  in the W-FA (Table S2 of the SM).

Finally, TGA results displayed mass losses at three different temperatures (100, 700, and 900 °C) for both FA and W-FA (Fig. 1e and f, respectively). The mass loss detected at 100 °C was related to the removal of humidity from the analysed samples, as also previously observed in the TGA results for cement. The mass losses observed at 700 and 900 °C, however, could be attributed to i) mass loss due to structural OH- groups from C-S-H gel (Gabrovšek et al., 2006), which might have formed during pre-washing, ii) the  $\text{CaCO}_3$  calcination reaction, and iii)  $\text{Ca}(\text{SO})_4$  degradation. In fact, according to the XRD data, both crystalline phases were observed in the FA before and after the washing pre-treatment (Fig. 1a and b, respectively).

### 3.3. The production of aggregates through single- and double-step pelletization

#### 3.3.1. Physical-chemical properties of aggregates

Through both single- and double-step pelletization methods the cold-bonding process led to aggregates with particle sizes ranging from 2 to 20 mm. In the case of single-step pelletization, the main particle size distribution was obtained between 4 and 16 mm, with percentages of 92.46%, 87.47%, and 86.90% for the S-C5S15 (Fig. 2a), S-C10S10, and S-C15S5 aggregates, respectively. In the case of the 2 mm particle size, S-C5S15 and S-C10S10 contained 0.24% and 1.64%, respectively (Fig. 2b). The resulting predominance of the 4–16 mm particles size range can be ascribable to the effect of the cold-bonding operating conditions involved (i.e. 45 rpm rotation and 45° plate inclination angle) on the coalescence phenomena of the loose materials (Ferraro et al., 2021). In fact, similar main particle size range was obtained in previous studies performing the cold-bonding process with equal plate rotation velocity and inclination angle values (Colangelo et al., 2015; Colangelo and Cioffi, 2013). On the contrary, no particle under 4 mm was obtained in the S-C15S5 aggregates, probably due to the higher amount of cement in the mixture, enabling better agglomeration of the FA particles. Accordingly, aggregates smaller than 4 mm were not considered for further characterization. As expected, double-step pelletization procedure generally led to the production of aggregates with a larger particle size, due to the formation of a second aggregate layer. The highest percentage of aggregates consisted of particles 16 mm

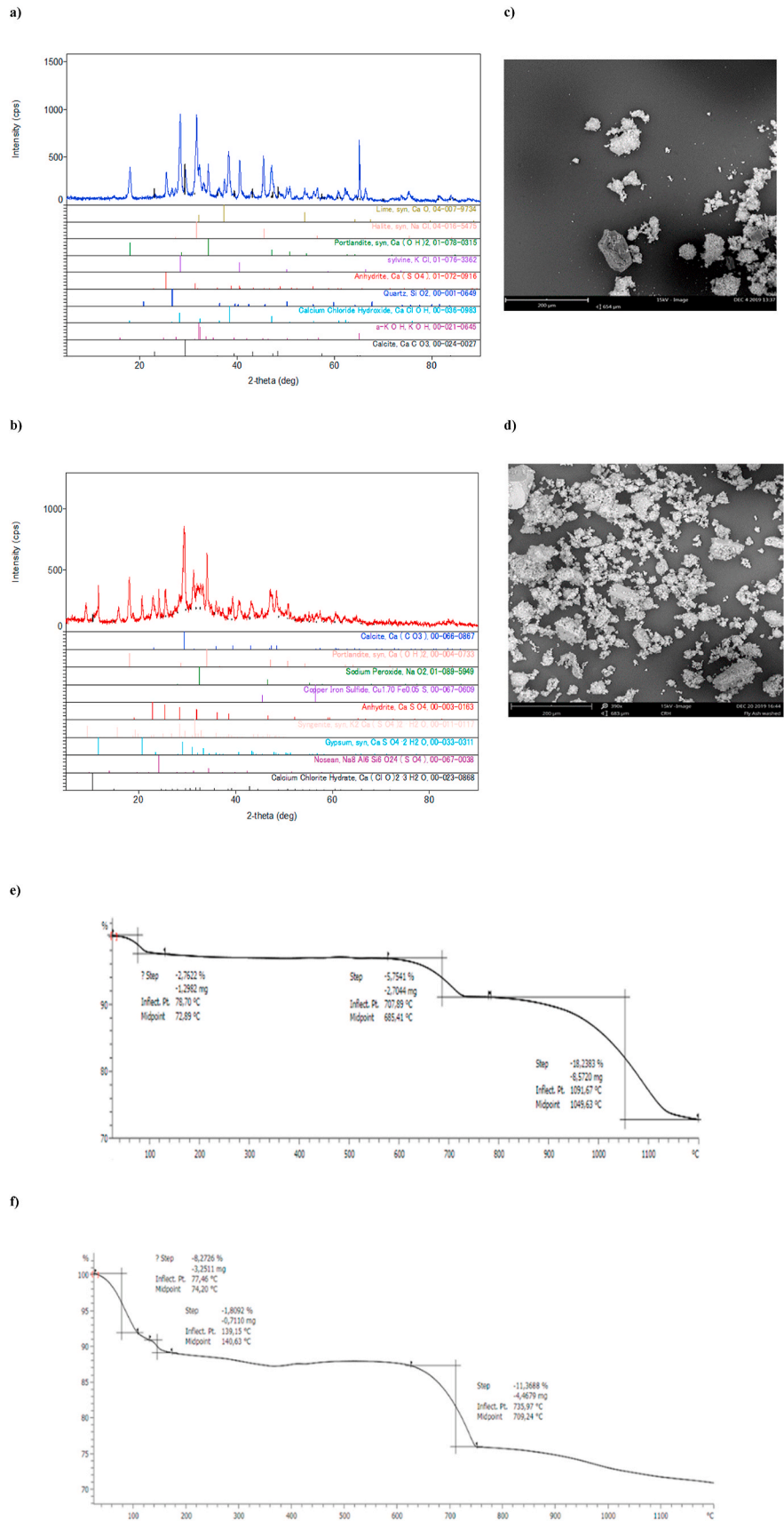


Fig. 1. XRD data for a) FA and b) W-FA, SEM scans for c) FA and d) W-FA, TGA data for e) FA and f) W-FA.



**Fig. 2.** Final specimens of a) S-C5S15, b) S-C10S10 (left side), S-C15S5 (right side), and c) D-C10S10 (left side), D-C15S5 (central), and D-C5S15 (right side) aggregates after the cold-bonding granulation process.

in size, with values equal to 8.61%, 18.99%, and 20.49% for D-C5S15, D-C10S10, and D-C15S5, respectively (Fig. 2c). Also in this case, no particles smaller than 4 mm were obtained for the D-C15S5 aggregates, while percentages equal to 4.55% and 2.53% were obtained for D-C5S15 and D-C10S10, respectively. Particles smaller than 4 mm from the double-step pelletization were not, however, further considered for proper comparison with aggregates from the single-step pelletization.

Data related to the WAC, density and open porosity of aggregates from single- and double-step pelletization are reported in Table 2, considering the lowest, average, and highest particle sizes (i.e. 4, 12.5, and 20 mm).

According to the results, at various particle sizes WAC values ranged between 16.66–18.18% and 8.55–15.48% in S-C5S15 and S-C10S10, respectively, with a generally observable decrease with increasing particle size (Baykal and Döven, 2000). The results observed are consistent with WAC values typical for commercial artificial aggregates, which range from 10 to 18% (Colangelo et al., 2015). A very high WAC value

(43.26%) was only observed in the 4 mm S-C15S5 aggregates, while acceptable WAC values were displayed in the same aggregate at both larger particle sizes (i.e. 12.5 and 20 mm). The highest WAC value observed for the 4 mm S-C15S5 aggregates also corresponded to the highest open porosity (69%) among the produced aggregates. This suggested that S-C15S5 aggregates at 4 mm size did not form with suitable mechanical characteristics during the cold-bonding process and further supported to not consider this particle size for the crushing strength determination. After the single-step pelletization, the density values of all the aggregates ranged between 1.57 and 1.85 g cm<sup>-3</sup>. These values allow the aggregates produced to be classified as LWAs, in accordance with the guidelines outlined in standard UNI EN 12620 (2013) (LWA density values from 1.4 to 2.4 g cm<sup>-3</sup>). The open porosity is an important factor affecting the mechanical characteristics and permeability of the aggregates. As already observed, except for the 4 mm particles of the S-C15S5 aggregates, an increase in the percentage of cement in the mixtures led to a decrease in the open porosity values. This

**Table 2**  
Physical-chemical and mechanical characteristics of aggregates from single- and double-step pelletization.

Aggregates	4 mm			12.5 mm				20 mm			
	WAC (%)	Density (g cm <sup>-3</sup> )	Open porosity (%)	WAC (%)	Density (g cm <sup>-3</sup> )	Open porosity (%)	Crushing strength (MPa)	WAC (%)	Density (g cm <sup>-3</sup> )	Open porosity (%)	Crushing strength (MPa)
S-C5S15	18.18	1.61	29.27	16.81	1.63	26.38	1.33	16.66	1.57	26.05	–
S-C10S10	8.55	1.85	15.79	15.48	1.63	25.20	1.45	11.96	1.69	20.19	1.42
S-C15S5	43.26	1.60	69	12.18	1.66	20.27	1.86	10.78	1.68	18.07	1.63
D-C5S15	11.40	1.73	19.74	11.50	1.76	20.33	1.95	9.22	1.74	16	–
D-C10S10	8.26	1.87	15.41	6.96	1.87	12.99	5.36	7.43	1.73	12.87	3.33
D-C15S5	21.63	1.75	38.43	15.51	1.63	25.29	10.92	9.99	1.67	16.72	10.94

could be correlated to the formation of a denser structure characterized by higher resistance to water absorption (Bui et al., 2012b). The porosity of the S-C5S15 and S-C10S10 aggregates, however, ranged from 18.07% to 29.7% in all particle sizes investigated.

The overall properties of the aggregates improved with double-step pelletization. The WAC values of D-C5S15, D-C10S10, and D-C15S5 aggregates were generally lower than those in the corresponding mixtures from single-step pelletization. The only exception observed was in the 12.5 mm D-C15S5 aggregates, which displayed a slightly higher WAC value (15.51%) compared to the S-C15S5 aggregates at the same particle size (12.18%). In the case of the D-C15S5 aggregates with a particle size of 4 mm, the highest WAC value among all mixtures (21.63%) was observed following the double-step pelletization. It is, however, worth noticing that the resulting WAC of the 4 mm S-C15S5 aggregates was twice as high than the corresponding value of the 4 mm D-C15S5 aggregates. The addition of a second layer led to an increase in aggregate density, which would be expected due to the presence of a higher amount of binder. Compared to the corresponding mixtures from the single-step pelletization process, slightly lower values were observed for the 12.5 and 20 mm particles in the D-C15S5 aggregates (1.63 and 1.67 g cm<sup>-3</sup>, respectively). Despite this, as also observed following the single-step pelletization, all the density values of the D-C5S15, D-C10S10, and D-C15S5 aggregates fell within the range to be classified as LWAs. Similarly to the WAC, a decrease in open porosity values was observed in the aggregates which underwent the double-step pelletization process. In most cases, the decrease in open porosity was significant compared to the corresponding mixtures from the single-step pelletization process, with the greatest reduction observed from 69% to 38.43% for the 4 mm S-C15S5 and D-C15S5 aggregates, respectively. In general, comparing the mixtures subjected to the double-step pelletization, the D-C10S10 aggregates were characterized by a lower WAC and open porosity, and a higher density compared to the D-C5S15 and D-C15S5 aggregates. This was true for almost all the particle sizes.

### 3.3.2. Mechanical properties of aggregates

Results from the tests determining the resistance of aggregates to impact varied according to the mixtures. The percentage of materials able to pass through a 2 mm sieve was 30.56%, 22.22%, and 25% for S-C5S15, S-C10S10, and S-C15S5 aggregates, respectively. Accordingly, the S-C10S10 aggregates showed the best performance, with the lowest 2 mm passing percentage. On the contrary, respective percentage values of 19.44%, 25%, and 44.44% were observed in D-C5S15, D-C10S10, and D-C15S5 aggregates, highlighting that the mixture with the lowest cement content in the first aggregate layer showed the highest impact resistance. The standard UNI EN 12620 (2013) classifies aggregates with a 2 mm passing percentage lower than 15% as very strong, aggregates with percentage values between 15 and 45% as suitable for road paving, and aggregates with percentage values higher than 45% as very weak. In accordance with this classification, the 2 mm passing percentage values displayed by all the aggregates investigated indicate their suitability for road paving.

Table 2 reports results regarding the crushing strength of aggregates with particle sizes of 12.5 and 20 mm, with the exception of the mixtures S-C5S15 and D-C5S15, which resulted in the lowest percentage of 20 mm particles produced (4.90 and 3.35%, respectively). An increase in the crushing strength of aggregates was observed in line with an increasing amount of binder (cement) following both single- and double-step pelletization. The latter result is expected, since the binder percentage represents the most significant parameter affecting the crushing strength property of aggregates (Tajra et al., 2018). At a particle size of 12 mm, the addition of a second layer (consisting of 70% MS and 30% cement) led to a higher crushing strength, with values for D-C5S15, D-C10S10, and D-C15S5 aggregates respectively 1.47, 3.70, and 5.87 times higher compared to the corresponding aggregates from the single-step pelletization process. With respect to the 20 mm particles, the D-C10S10 and D-C15S5 aggregates displayed values of crushing

strength 2.35 and 6.71 times higher than S-C10S10 and S-C15S5, respectively. The values of crushing strength for the aggregates produced by single-step pelletization, and the D-C5S15 mixture, on the other hand, were generally lower than 2 MPa. This latter result could be strongly dependent on the chemical composition of the W-FA involved in the production of the aggregates. In particular, a high CaO content (39.90 wt%) was detected in the W-FA of this study, which generally displays a negative impact on the crushing strength of aggregates (Gesoğlu et al., 2007).

Nonetheless, the addition of a second layer in the D-C10S10 and D-C15S5 aggregates resulted in a significant increase in crushing strength, with results comparable to values shown in the literature (almost 6 MPa) for LWAs produced from a mixture of FA, cement, and GBFS (Hwang and Tran, 2015). Moreover, the crushing strength of the D-C15S5 aggregates was slightly lower than LWAs made by FA and GBFS with the addition of alkali activators (almost 15 MPa) (Bui et al., 2012a), but higher than aggregates made from different mixtures of FA and cement (6.01–8.57 MPa) (Chi et al., 2003).

### 3.4. Microstructural evaluation

X-ray micro-CT was used to reconstruct the 3D internal pore structure and to determine overall porosity. The inner structures observed differed between mixtures, as can be seen from the values reported in Table 3, as well as from the results of X-ray micro-CT on aggregates from single- and double-step pelletization (Fig. 3a and b, respectively) and LV SEM analysis (Fig. 4).

In the aggregates subjected to double-step pelletization, decreases in the overall porosity and number of pores were observed with an increasing amount of cement, and a similar trend was observed for aggregates produced from single-step pelletization.

The majority of pores were smaller than 0.5 mm in diameter for all the samples. However, the higher overall porosity values reported (ranging from 32.99 to 45.12%) can also be attributed to the presence of some larger pores or empty spaces (with a diameter greater than 0.5 mm). Fig. 4a and b show voids alongside the additional layers in the D-C10S10 and D-C5S15 aggregates, respectively, as a result of the double-step pelletization. Nevertheless, a thicker second layer is observed in the D-C10S10 aggregates compared to D-C5S15 ones, which is expected due to the presence of a higher amount of binder in the first group of aggregates compared to the latter. On the contrary, a compact and dense structure was displayed in the D-C15S5 aggregates, with a well bonded outer layer (Fig. 4c and d). This was consistent with the better mechanical characteristics (Table 2) observed in this mixture, which further confirms that the wastes:binder mixture involved for the production of D-C15S5 aggregates was the optimal solution for the double-step pelletization process.

In half of the granules, porosity and pore size distribution were also determined by MIP (Table 3). Porosity evaluated by MIP is significantly higher than that obtained by X-ray micro-CT, which is attributed to differences in resolution between the two methods. In fact, while X-ray micro-CT only recognizes pores above 15 µm, the resolution of MIP can measure as low as few nm. The trend, however, is the same as observed by micro-CT displaying porosity decrease with an increasing amount of cement. According to the results from Fig. 5, it can be seen that the pore

**Table 3**  
Structural characteristics of samples, as determined by X-ray micro-CT and MIP.

Aggregates	Number of pores by X-ray micro-CT	Overall porosity (%) by X-ray micro-CT	Porosity (%) by MIP
S-C5S15	17050	22.56	45.12
S-C10S10	17445	18.55	34.12
S-C15S5	11494	13.76	35.85
D-C5S15	61035	21.07	36.62
D-C10S10	41612	16.71	32.99
D-C15S5	13835	20.69	37.66

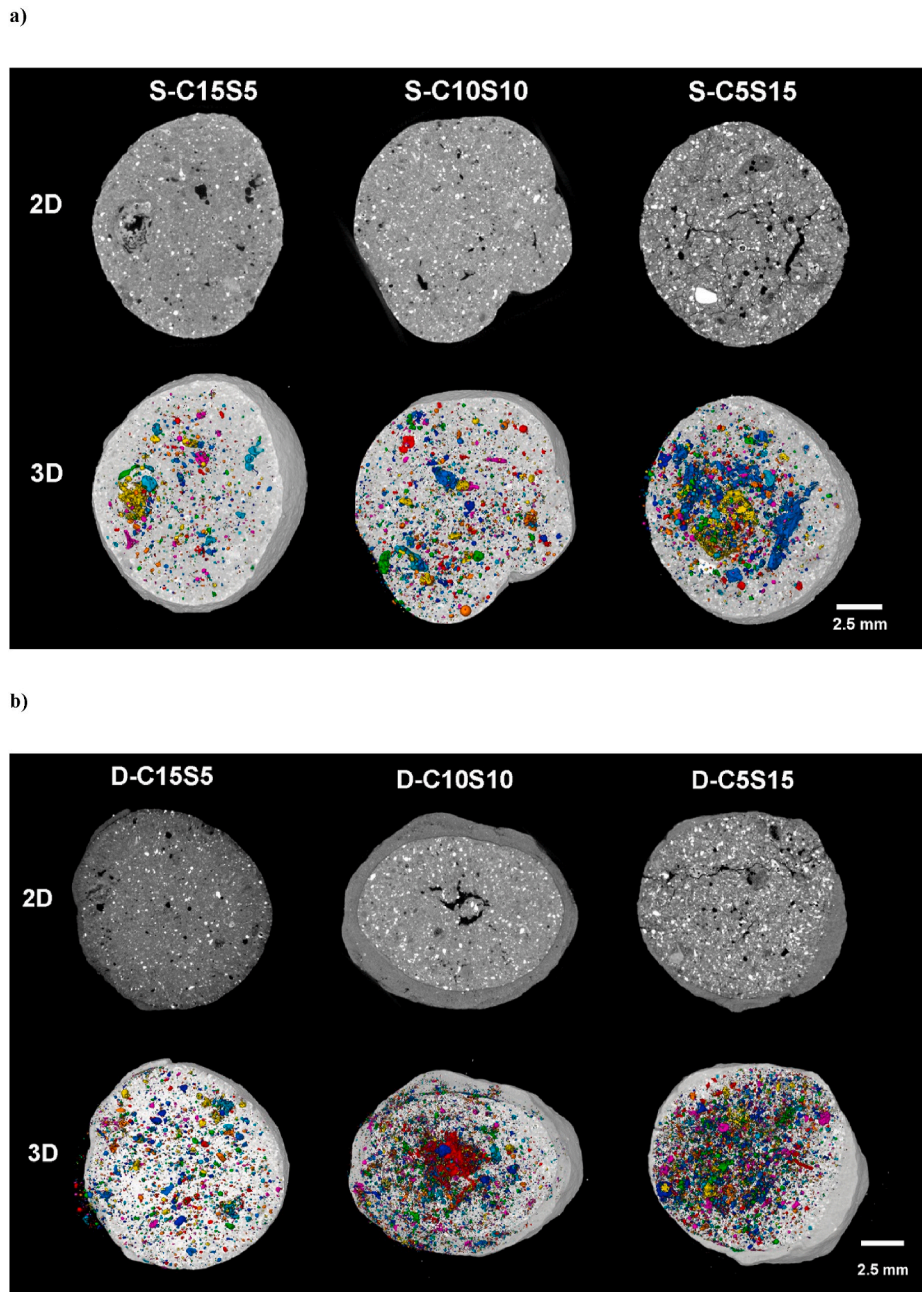


Fig. 3. Internal pore structure of samples after a) single-step pelletization, and b) double-step pelletization, as determined by X-ray micro-CT.

diameter was below  $1\ \mu\text{m}$  in the majority of aggregates for all the cases, with the exception of the S-C5S15 sample.

### 3.5. Leaching tests

Table 4 reports results related to the release of HMs, chloride and sulphate in aggregates from both single- and double-step pelletization, and the related limit values for non-hazardous wastes. Accounting for the results of the HMs concentration in the leachate, in all the aggregates a null release was only observed for Cu. The concentration values of all the HMs were within the limits for non-hazardous materials, as reported by the UNI EN 10802 (2013). In general, a lower release of HMs was observed in the aggregates which underwent double-step pelletization compared to the corresponding aggregates produced by the single-step pelletization. This was consistent with the lower porosity values of the aggregates observed after the addition of a second layer. Higher leaching

occurred in the D-C5S15 and D-C10S10 aggregates compared to S-C5S15 and S-C10S10 only in the case of Cr. Moreover, comparing the aggregates produced from double-step pelletization, the best performance in terms of limited leaching varied between the different aggregates as a function of the HM considered.

On the contrary, the leaching values of chloride and sulphate were over the limits in almost all aggregates, the only exception being the D-C10S10 aggregates where the resulting sulphate concentration was under the limit. Also in this case, however, the addition of a second layer displayed beneficial effects, resulting in a release rate 1.73–4.02 times lower in the case of chloride and 1.58–5.67 times lower for sulphate. Accordingly, the double-step pelletization can already represent a strategy for the process efficiency enhancement in terms of safe aggregates production. Indeed, leaching results about chloride and sulphate after cold-bonding stabilization clearly indicate that future research activities aimed at improving these elements release containment should

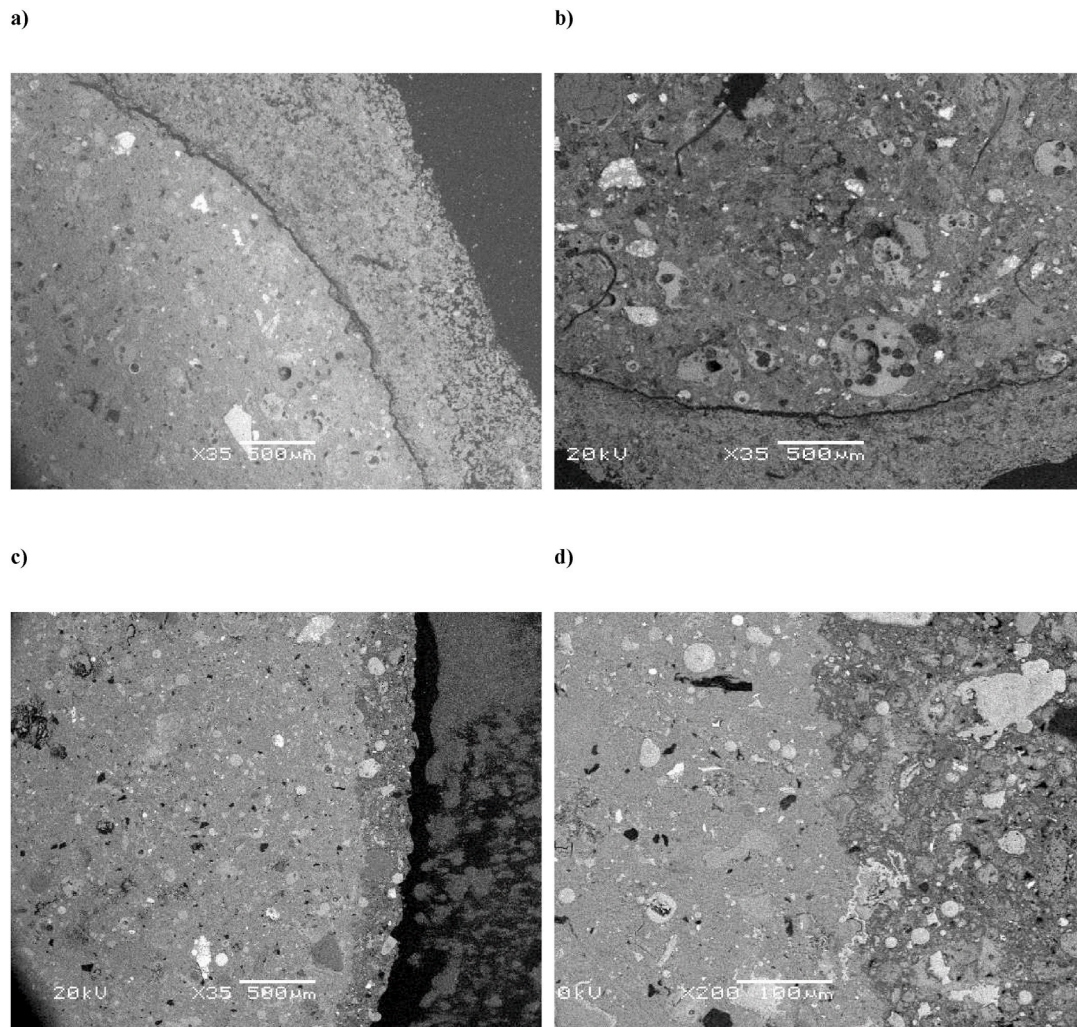


Fig. 4. LV SEM of a) D-C10S10 aggregates at 50x magnification, b) D-C5S15 aggregates at 35x magnification, and D-C15S5 aggregates at c) 50x and d) 200x magnification.

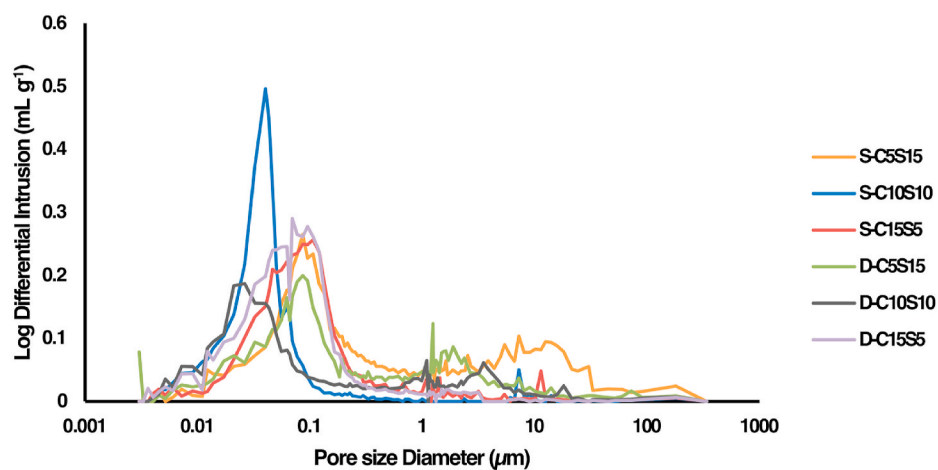


Fig. 5. Pore size distribution of aggregates, as determined by MIP analysis.

be further deepened. For instance, these aggregates could undergo to a post-washing treatment aimed at further decreasing the leachable amount of chloride and sulphate. The latter could be integrated in pre-washing and S/S techniques studied in this work in order to provide a complete treatment strategy. Indeed, the effluents from both pre- and

post-washing processes should require a suitable treatment for the further reuse/disposal of the washing solutions. An example is provided by the dehydration of the washing solution in order to produce organic salts. Further potential strategy could be represented by the involvement of reverse osmosis (RO) to demineralize the total washing solution, thus

**Table 4**

Release of HMs, chloride, and sulphate in aggregates from single- and double-step pelletization and the related limit values for non-hazardous wastes.

Aggregates	Cu (mg L <sup>-1</sup> )	Pb (mg L <sup>-1</sup> )	Zn (mg L <sup>-1</sup> )	Cd (mg L <sup>-1</sup> )	Cr (mg L <sup>-1</sup> )	Chloride (mg L <sup>-1</sup> )	Sulphate (mg L <sup>-1</sup> )
S-C5S15	0	1.15	1.11	0.01	0.45	39439	7283
S-C10S10	0	0	0.28	0.04	0.1	22930	5158
S-C15S5	0	0.71	0.32	0.06	0.55	22996	14859
D-C5S15	0	0.49	0.62	0.03	0.49	9819	4601
D-C10S10	0	0	0.17	0.01	0.35	7101	909
D-C15S5	0	0.24	0.29	0	0.53	13333	3595
Legislative limits <sup>a</sup>	5	1	5	0.1	1	1500	2000

<sup>a</sup> Italian regulation limit values for disposal of stabilized waste in non-hazardous waste landfill (D.M. September 27, 2010, 2010).

allowing its reuse in further washing steps for both FA and aggregates. Also in this case, in view of a circular economy perspective, the brines resulting from RO could be reused for the production of inorganic salts, as also reported in several literature works (Jiang et al., 2014; Pérez-González et al., 2012; Sorour et al., 2015). Then, based on their composition, the produced inorganic salts could be either used as de-icing salts for ice and snow removal or disposed if the chemical characteristics are not suitable for their application.

Despite this, a proper evaluation on the practical suitability of the investigated approach should be based on a comprehensive assessment of all the related technical aspects. In fact, the cold-bonding process presented in this work proved to be effective in the production of aggregates with proper mechanical characteristics if optimal mixture composition is appropriately selected. Moreover, it is worth noticing that efficient HMs stabilization was achieved also after the single-step pelletization. These further considerations generally suggest that cold-bonding process has potential applicability as S/S technique for FA treatment and resulting aggregates production. Then, future scientific efforts should be aimed at finding technical enhancement (such as involvement of different waste materials in the aggregates mixture, operating parameters optimization of FA pre-treatment, etc.). This could provide a practical solution to improve the reliability of cold-bonding process for the production of sustainable and environmentally safe aggregates.

#### 4. Conclusions

The present work focused on a remediation procedure for hazardous MSWI FA. The first step entailed washing pre-treatment of the FA with water, which resulted in a significant decrease in the content of soluble salts (chlorides and sulphates). This was confirmed by XRF and XRD analysis, which respectively reported a reduction in the presence of elements related to chlorides and sulphates, as well as a lower content of chlorine crystalline phases. Accordingly, the effect of the washing pre-treatment was beneficial for the removal of elements that could hinder the efficiency of a further stabilization process. The second step was carried out on W-FA by means of a cold-bonding pelletization process for the production of aggregates. A comparison of the characteristics of the aggregates produced from single- and double-step pelletization highlighted the benefit of a second aggregate layer, which improved both the physical-chemical properties (WAC, density, and open porosity) and crushing strength of the aggregates. This proves the efficacy of using various wastes in the production of aggregates through the process of double-step pelletization in order to potentially achieve leaching elements reduction under regulation limits through effective strategies. Moreover, it should be also taken into account that the aggregates obtained through cold-bonding cannot be directly used as end of waste. In fact, they generally need a further processing in a waste treatment plant to be transformed in a second raw material before their reuse. In this

way, the obtained product can be suitable to be employed as artificial aggregates for concrete. These considerations provide interesting perspectives for future studies aimed at identifying a complete treatment chain (comprehensive of pre- and post-treatment) to further improve the characteristics of aggregates prior to their reuse.

#### Statement of novelty

Existing literature investigates the cold-bonding granulation for municipal solid waste incineration fly-ash focusing on binder and waste typologies addition in the aggregate mix-design. This work deepens several process key-points including the fly-ash pre-treatment and the aggregates manufacture through single- and double-step pelletization approaches. The latter represents a novel and useful research contribution since improved mechanical properties and enhanced waste reuse can be achieved by second aggregate layer addition. Fly-ash represents a hazardous waste for the chemical-reactivity and high heavy metals, sulphates and chlorides content. Indeed, these characteristics corroborate the concernment about the deriving risks for the environment and organisms health.

#### CRedit authorship contribution statement

**Alberto Ferraro:** Conceptualization, Writing – original draft. **Vilma Ducman:** Conceptualization, Formal analysis, Supervision. **Francesco Colangelo:** Methodology, Formal analysis. **Lidija Korat:** Methodology. **Danilo Spasiano:** Methodology, Writing – review & editing. **Ilenia Farina:** Writing – review & editing, Supervision.

#### Declaration of competing interest

The authors declare that they have no known competing financial interests or personal relationships that could have appeared to influence the work reported in this paper.

#### Data availability

Data will be made available on request.

#### Acknowledgments

The authors would like to thank Eng. Luigi Pugliese and Eng. Marco Valerio Pinto for their valuable support in performing experiments. Vilma Ducman and Lidija Korat would like to acknowledge financial support from the Slovenian Research Agency Programme Group P2-0273. Francesco Colangelo would like to thank the Italian Ministry of University and Research for the support through the PRIN 2020 grant number 2020WFEFKX5.

#### Appendix A. Supplementary data

Supplementary data to this article can be found online at <https://doi.org/10.1016/j.jclepro.2022.135275>.

#### References

- Ayati, B., Ferrándiz-Mas, V., Newport, D., Cheeseman, C., 2018. Use of clay in the manufacture of lightweight aggregate. *Construct. Build. Mater.* 162, 124–131. <https://doi.org/10.1016/j.conbuildmat.2017.12.018>.
- Barjoveanu, G., de Gisi, S., Casale, R., Todaro, F., Notarnicola, M., Teodosiu, C., 2018. A life cycle assessment study on the stabilization/solidification treatment processes for contaminated marine sediments. *J. Clean. Prod.* 201, 391–402. <https://doi.org/10.1016/j.jclepro.2018.08.053>.
- Baykal, G., Döven, A.G., 2000. Utilization of fly ash by pelletization process; theory, application areas and research results. *Resour. Conserv. Recycl.* 30, 59–77. [https://doi.org/10.1016/S0921-3449\(00\)00042-2](https://doi.org/10.1016/S0921-3449(00)00042-2).
- Bui, L.A., Hwang, C., Chen, C., Hsieh, M., 2012a. Characteristics of cold-bonded lightweight Aggregate produced with different mineral admixtures. *Appl. Mech.*

- Mater. 174–177, 978–983. <https://doi.org/10.4028/www.scientific.net/amm.174-177.978>.
- Bui, L.A., Hwang, C., Chen, C., Lin, K., Hsieh, M., 2012b. Manufacture and performance of cold bonded lightweight aggregate using alkaline activators for high performance concrete. *Construct. Build. Mater.* 35, 1056–1062. <https://doi.org/10.1016/j.conbuildmat.2012.04.032>.
- Chi, J.M., Huang, R., Yang, C.C., Chang, J.J., 2003. Effect of aggregate properties on the strength and stiffness of lightweight concrete. *Cement Concr. Compos.* 25, 197–205. [https://doi.org/10.1016/S0958-9465\(02\)00020-3](https://doi.org/10.1016/S0958-9465(02)00020-3).
- Colangelo, F., Cioffi, R., 2013. Use of cement kiln dust, blast furnace slag and marble sludge in the manufacture of sustainable artificial aggregates by means of cold bonding pelletization. *Materials* 6, 3139–3159. <https://doi.org/10.3390/ma6083139>.
- Colangelo, F., Cioffi, R., Montagnaro, F., Santoro, L., 2012. Soluble salt removal from MSWI fly ash and its stabilization for safer disposal and recovery as road basement material. *Waste Manag.* 32, 1179–1185. <https://doi.org/10.1016/j.wasman.2011.12.013>.
- Colangelo, F., Messina, F., Cioffi, R., 2015. Recycling of MSWI fly ash by means of cementitious double step cold bonding pelletization: technological assessment for the production of lightweight artificial aggregates. *J. Hazard Mater.* 299, 181–191. <https://doi.org/10.1016/j.jhazmat.2015.06.018>.
- de Gisi, S., Chiarelli, A., Tagliente, L., Notarnicola, M., 2018. Energy, environmental and operation aspects of a SRF-fired fluidized bed waste-to-energy plant. *Waste Manag.* 73, 271–286. <https://doi.org/10.1016/j.wasman.2017.04.044>.
- Ferone, C., Colangelo, F., Messina, F., Iucolano, F., Liguori, B., Cioffi, R., 2013. Coal combustion wastes reuse in low energy artificial aggregates manufacturing. *Materials* 6, 5000–5015. <https://doi.org/10.3390/ma6115000>.
- Ferraro, A., Colangelo, F., Farina, I., Race, M., Cioffi, R., Cheeseman, C., Fabbricino, M., 2021. Cold-bonding process for treatment and reuse of waste materials: technical designs and applications of pelletized products. *Crit. Rev. Environ. Sci. Technol.* 51, 2197–2231. <https://doi.org/10.1080/10643389.2020.1776052>.
- Ferraro, A., Farina, I., Race, M., Colangelo, F., Cioffi, R., Fabbricino, M., 2019. Pre-treatments of MSWI fly-ashes: a comprehensive review to determine optimal conditions for their reuse and/or environmentally sustainable disposal. *Rev. Environ. Sci. Biotechnol.* 18, 453–471. <https://doi.org/10.1007/s11157-019-09504-1>.
- Franković, A., Bosiljkov, V.B., Ducman, V., 2017. Lightweight aggregates made from fly ash using the cold-bond process and their use in lightweight concrete. *Materiali in Tehnologije* 51, 267–274. <https://doi.org/10.17222/mit.2015.337>.
- Gabrovsek, R., Vuk, T., Kaučić, V., 2006. Evaluation of the hydration of portland cement containing various carbonates by means of thermal analysis. *Acta Chim. Slov.* 53, 159–165.
- Gesoğlu, M., Özturan, T., Güneyisi, E., 2007. Effects of fly ash properties on characteristics of cold-bonded fly ash lightweight aggregates. *Construct. Build. Mater.* 21, 1869–1878. <https://doi.org/10.1016/j.conbuildmat.2006.05.038>.
- Hu, Y., Zhang, P., Li, J., Chen, D., 2015. Stabilization and separation of heavy metals in incineration fly ash during the hydrothermal treatment process. *J. Hazard Mater.* 299, 149–157. <https://doi.org/10.1016/j.jhazmat.2015.06.002>.
- Hwang, C.L., Tran, V.A., 2015. A study of the properties of foamed lightweight aggregate for self-consolidating concrete. *Construct. Build. Mater.* 87, 78–85. <https://doi.org/10.1016/j.conbuildmat.2015.03.108>.
- Jiang, C., Wang, Y., Zhang, Z., Xu, T., 2014. Electrodialysis of concentrated brine from RO plant to produce coarse salt and freshwater. *J. Membr. Sci.* 450, 323–330. <https://doi.org/10.1016/j.memsci.2013.09.020>.
- Kirkelund, G.M., Skevi, L., Ottosen, L.M., 2020. Electrodialytically treated MSWI fly ash use in clay bricks. *Construct. Build. Mater.* 254, 119286. <https://doi.org/10.1016/j.conbuildmat.2020.119286>.
- Korat, L., Ducman, V., Legat, A., Mirtič, B., 2013. Characterisation of the pore-forming process in lightweight aggregate based on silica sludge by means of X-ray microtomography (micro-CT) and mercury intrusion porosimetry (MIP). *Ceram. Int.* 39, 6997–7005. <https://doi.org/10.1016/j.ceramint.2013.02.037>.
- Loginova, E., Proskurnin, M., Brouwers, H.J.H., 2019. Municipal solid waste incineration (MSWI) fly ash composition analysis: a case study of combined chelant-based washing treatment efficiency. *J. Environ. Manag.* 235, 480–488. <https://doi.org/10.1016/j.jenvman.2019.01.096>.
- Makarichi, L., Jutidamrongphan, W., Techato, K., 2018. The evolution of waste-to-energy incineration: a review. *Renew. Sustain. Energy Rev.* 91, 812–821. <https://doi.org/10.1016/j.rser.2018.04.088>.
- Malenšek, N., Ducman, V., Mirtič, B., 2015. Recycled granulate obtained from waste alumina-rich refractory powder by the cold bonding process. *Ceram. Int.* 41, 8996–9002. <https://doi.org/10.1016/j.ceramint.2015.03.214>.
- Manikandan, R., Ramamurthy, K., 2007. Influence of fineness of fly ash on the aggregate pelletization process. *Cement Concr. Compos.* 29, 456–464. <https://doi.org/10.1016/j.cemconcomp.2007.01.002>.
- Pérez-González, A., Urriaga, A.M., Ibáñez, R., Ortiz, I., 2012. State of the art and review on the treatment technologies of water reverse osmosis concentrates. *Water Res.* 46, 267–283. <https://doi.org/10.1016/j.watres.2011.10.046>.
- Perumal, G., Sivakumar, A., 2014. Performance evaluation of alkali activated fly ash lightweight aggregates. *Eng. J.* 18, 77–85. <https://doi.org/10.4186/ej.2014.18.1.77>.
- Race, M., 2017. Applicability of alkaline precipitation for the recovery of EDDS spent solution. *J. Environ. Manag.* 203, 358–363. <https://doi.org/10.1016/j.jenvman.2017.08.013>.
- Rehman, M.U., Rashid, K., Haq, E.U., Hussain, M., Shehzad, N., 2020. Physico-mechanical performance and durability of artificial lightweight aggregates synthesized by cementing and geopolymerization. *Construct. Build. Mater.* 232, 117290. <https://doi.org/10.1016/j.conbuildmat.2019.117290>.
- Senneca, O., Cortese, L., di Martino, R., Fabbricino, M., Ferraro, A., Race, M., Scopino, A., 2020. Mechanisms affecting the delayed efficiency of cement based stabilization/solidification processes. *J. Clean. Prod.* 261, 121230. <https://doi.org/10.1016/j.jclepro.2020.121230>.
- Sorour, M.H., Hani, H.A., Shaalan, H.F., Al-Bazedi, G.A., 2015. Schemes for salt recovery from seawater and RO brines using chemical precipitation. *Desalination Water Treat.* 55, 2398–2407. <https://doi.org/10.1080/19443994.2014.946720>.
- Tajra, F., Elrahman, M.A., Chung, S.Y., Stephan, D., 2018. Performance assessment of core-shell structured lightweight aggregate produced by cold bonding pelletization process. *Construct. Build. Mater.* 179, 220–231. <https://doi.org/10.1016/j.conbuildmat.2018.05.237>.
- Tang, P., Brouwers, H.J.H., 2017. Integral recycling of municipal solid waste incineration (MSWI) bottom ash fines (0–2 mm) and industrial powder wastes by cold-bonding pelletization. *Waste Manag.* 62, 125–138. <https://doi.org/10.1016/j.wasman.2017.02.028>.
- Thomas, J., Harilal, B., 2015. Properties of cold bonded quarry dust coarse aggregates and its use in concrete. *Cement Concr. Compos.* 62, 67–75. <https://doi.org/10.1016/j.cemconcomp.2015.05.005>.
- UNI EN 197-1, 2011. *Cement - Part 1: Composition, Specifications and Conformity Criteria for Common Cements*.
- UNI EN 933-1, 2012. *Tests for Geometrical Properties of Aggregates - Part 1: Determination of Particle Size Distribution - Sieving Method*.
- UNI EN 10802, 2013. *Waste - Manual Sampling, Sample Preparation and Analysis of Eluates*.
- UNI EN 12620, 2013. *Aggregates for Concrete*.
- UNI EN 13055-1, 2002. *Lightweight Aggregates - Part 1: Lightweight Aggregates for Concrete, Mortar and Grout*.
- Valia, K.S., Murugan, S.B., 2020. Effect of different binders on cold-bonded artificial lightweight aggregate properties. *Advances in Concrete Construction* 9, 183–193.
- Xinghua, H., Shujing, Z., Hwang, J.-Y., 2016. Physical and chemical properties of MSWI fly ash. In: Ikhmayies, S.J., Li, B., Carpenter, J.S., Hwang, Jiann-Yang, Monteiro, S. N., Li, J., Firrao, D., Zhang, M., Peng, Z., Escobedo-Diaz, J.P., Bai, C. (Eds.), *Characterization of Minerals, Metals, and Materials*. Springer, Cham, pp. 451–459. [https://doi.org/10.1007/978-3-319-48210-1\\_56](https://doi.org/10.1007/978-3-319-48210-1_56).
- Yang, Z., Tian, S., Ji, R., Liu, L., Wang, X., Zhang, Z., 2017. Effect of water-washing on the co-removal of chlorine and heavy metals in air pollution control residue from MSW incineration. *Waste Manag.* 68, 221–231. <https://doi.org/10.1016/j.wasman.2017.06.039>.
- Zheng, L., Wang, C., Wang, W., Shi, Y., Gao, X., 2011. Immobilization of MSWI fly ash through geopolymerization: effects of water-wash. *Waste Manag.* 31, 311–317. <https://doi.org/10.1016/j.wasman.2010.05.015>.